AFRL-SN-RS-TR-1998-3
Final Technical Report
March 1998

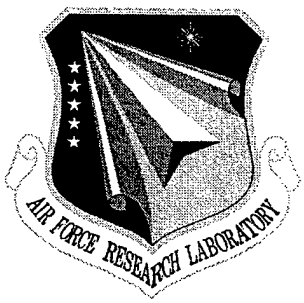

MECHANISM AND OPTIMUM DEMODULATION SCHEME FOR FREQUENCY-MODULATED FEEDBACK SUSTAINED PULSATIONS IN LASER DIODES

Rochester Institute of Technology

Guifang Li

APPROVED FOR PUBLIC RELEASE; DISTRIBUTION UNLIMITED.

AIR FORCE RESEARCH LABORATORY
SENSORS DIRECTORATE
ROME RESEARCH SITE
ROME, NEW YORK

This report has been reviewed by the Air Force Research Laboratory, Information Directorate, Public Affairs Office (IFOIPA) and is releasable to the National Technical Information Service (NTIS). At NTIS it will be releasable to the general public, including foreign nations.

AFRL-SN-RS-TR-1998-3 has been reviewed and is approved for publication.

APPROVED: David Grucza
DAVID GRUCZA
Project Engineer

FOR THE DIRECTOR: Gary D. Barmore
GARY D. BARMORE, Maj, USAF
Chief, Rome Operations Office
Sensors Directorate

If your address has changed or if you wish to be removed from the Air Force Research Laboratory Rome Research Site mailing list, or if the addressee is no longer employed by your organization, please notify AFRL/SNDP, 25 Electronic Pky, Rome, NY 13441-4515. This will assist us in maintaining a current mailing list.

Do not return copies of this report unless contractual obligations or notices on a specific document require that it be returned.

REPORT DOCUMENTATION PAGE			Form Approved OMB No. 0704-0188

1. AGENCY USE ONLY *(Leave blank)*	2. REPORT DATE	3. REPORT TYPE AND DATES COVERED
	March 1998	Final Mar 96 - Sep 97

4. TITLE AND SUBTITLE
MECHANISM AND OPTIMUM DEMODULATION SCHEME FOR FREQUENCY-MODULATED FEEDBACK SUSTAINED PULSATIONS IN LASER DIODES

5. FUNDING NUMBERS
C - F30602-96-2-0032
PE - 62702F
PR - 4600
TA - P5
WU - PE

6. AUTHOR(S)
Guifang Li

7. PERFORMING ORGANIZATION NAME(S) AND ADDRESS(ES)
Rochester Institute of Technology
One Lomb Memorial Drive
Rochester NY 14623-5604

8. PERFORMING ORGANIZATION REPORT NUMBER
N/A

9. SPONSORING/MONITORING AGENCY NAME(S) AND ADDRESS(ES)
Air Force Research Laboratory/SNDP
25 Electronic Pky
Rome NY 13441-4515

10. SPONSORING/MONITORING AGENCY REPORT NUMBER
AFRL-SN-RS-TR-1998-3

11. SUPPLEMENTARY NOTES
Air Force Research Laboratory Project Engineer: David J. Grucza/SNDP/(315) 330-2105

12a. DISTRIBUTION AVAILABILITY STATEMENT
Approved for public release; distribution unlimited.

12b. DISTRIBUTION CODE

13. ABSTRACT *(Maximum 200 words)*
The operation regimes and dynamic properties of semiconductor laser diodes are significantly affected by external feedback. Investigation of the dynamics of Self-Sustained Pulsation (SSP) in the semiconductor laser diodes with optoelectronic feedback is presented. The laser diode (LD) is assumed to be a noiseless two-section Fabry-Perot laser diode with linear gain in both sections. The feedback is assumed to consist of a photodetector and wide-band band-pass microwave amplifier. For a certain range of the laser diode and feedback parameters the system undergoes high-frequency (about 1GHz) oscillations resulting from structural instability in system dynamics. Frequency, amplitude and other parameters of Self-Sustained Pulsation are electrically tunable. The system dynamics are investigated from the standpoint of stability analysis as well as direct numerical simulation. The stability analysis performed shows that for certain laser diode and operating/feedback parameters, the laser diode/feedback system exhibits an instability which results in self-sustained pulsation.

14. SUBJECT TERMS	15. NUMBER OF PAGES
Laser Diodes, Optical Communications, Nonlinear Dynamics, Subcarrier Multiplexing	40
	16. PRICE CODE

17. SECURITY CLASSIFICATION OF REPORT	18. SECURITY CLASSIFICATION OF THIS PAGE	19. SECURITY CLASSIFICATION OF ABSTRACT	20. LIMITATION OF ABSTRACT
UNCLASSIFIED	UNCLASSIFIED	UNCLASSIFIED	UL

Table of Contents

List of Figures

Abstract

The operation regimes and dynamic properties of semiconductor laser diodes are significantly affected by external feedback. Investigation of the dynamics of Self-Sustained Pulsation (SSP) in semiconductor laser diodes with optoelectronic feedback is presented. The laser diode (LD) is assumed to be a noiseless two-sectional Fabry-Perot laser diode with linear gain in both sections. The feedback is assumed to consist of a photodetector and wide-band band-pass microwave amplifier. For a certain range of the laser diode and feedback parameters the system undergoes high-frequency (about 1GHz) oscillations resulting from structural instability in system dynamics. Frequency, amplitude and other parameters of Self-Sustained Pulsation are electrically tunable. The system dynamics are investigated from the standpoint of stability analysis as well as direct numerical simulation. The amplitude modulated microwave/millimeter wave oscillations can be used in high-speed optical communication networks.

1. Introduction

Self-Sustained Pulsation (SSP) is a well known and intensely studied phenomenon observed in semiconductor laser diodes (LD). Under certain conditions operation of a laser diode becomes unstable and then undergoes SSP. In SSP the optical field intensity inside the laser cavity, output power and other dynamic characteristics of the laser exhibit periodic changes in time. Usually these changes have the form of a pulse train consisting of short sharp peaks [1], [2], [3].

Repetition rate, duration and, to a certain extent, shape of these pulses can be electrically tuned by an appropriate choice of the operation regime of the laser system [1], [2]. These SSP parameters also exhibit strong dependence upon certain parameters of the LD itself. LD parameter such as carrier lifetime, cavity loss rate, refraction index of the laser medium etc affect the SSP. SSP laser diodes have been considered for several promising practical applications. Recently the self-pulsing LDs have been proposed for use as sources of subcarriers for lightwave communication networks. Subcarrier multiplexing is supposed to be compatible with wavelength-division multiplexing and extend the capacity of WDM networks. Both analog (up to 1 GHz) [1] and digital (up to 800 Mb/s) [5] transmission with SSP subcarriers have been reported. High repetition rate pulse trains generated by self-pulsing LDs can also be used in time-division multiplexing (TDM) digital communication networks for bit representation.

The origin of SSP is the presence of certain kind of instability in the dynamics of laser diodes. The physical nature of SSP can be understood on the basis of mathematical modeling of LD dynamics. SSP is essentially a nonlinear phenomenon and requires applying techniques of nonlinear system theory to the basic dynamic equations of semiconductor lasers. The standard approach involved in such a modeling is based on use of rate equations for the semiconductor LD modified so they account for possible instabilities in the laser dynamics.

One of the models utilized in this approach is presented in [1] and describes SSP occurring in spatially inhomogeneous LDs. Spatial variation of parameters of the laser medium is taken into account by use of a two-sectional approximation, which assumes

that the LD consists of two sections filled with the active media with different amplification/absorption properties, i. e. different values and/or sign of the medium gain.

In this paper the theoretical approach developed in [1] is extended and used to investigate dynamics for SSP in two-sectional LDs with optoelectronic feedback. The two-sectional laser diode (TSLD) is looked at as a nonlinear system characterized by rate equations, which can be used as state equations for the analysis of the nonlinear dynamics.

In following we focus first on a theoretical discussion based on linearized rate equations for the two-sectional model. Analysis of this kind provides means to determine whether or not SSP occurs in the system with a certain given set of parameter values, to predict the boundaries of the SSP-region in parameter space, and to give (in certain simple cases) estimates for SSP frequency.

Furthermore, we use the computer simulation of the TSLD with optoelectronic feedback with practically achievable parameters to prove the existence of SSP, measure its frequency and amplitude, observe the effect of the feedback delay on them and study amplitude modulated SSP.

2. Theory

2.1 Rate equations and stability analysis

In order to investigate two-sectional laser diodes with optoelectronic feedback we make use of rate equations presented in [1] modified so they account for optoelectronic feedback. The schematic of the system is shown in Fig. 1. Each section of TSLD has it's own feedback loop consisting of photodetector PD and bandpass feedback amplifiers FBA(A) or FBA(B). The output current of the feedback amplifiers is fed back to current terminals of the TSLD, contributing to the total injection current.

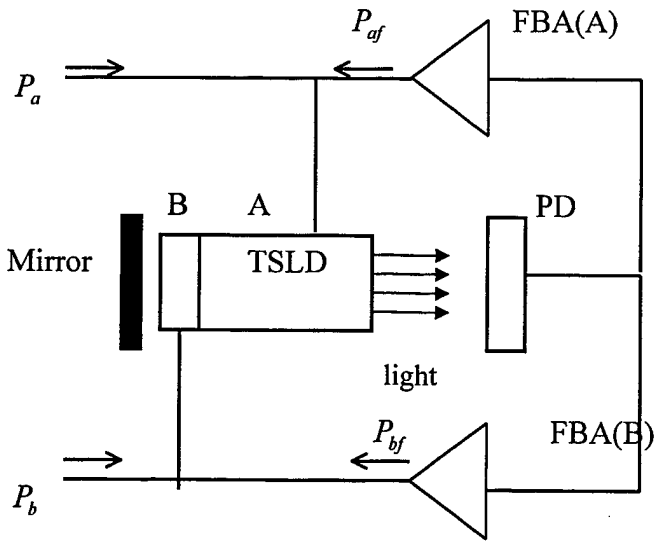

Fig. 1 Schematics of TSLD with optoelectronic feedback.

The rate equations for the two-sectional system with an optical feedback are as follows:

$$\frac{dn_a}{dt} = -\frac{n_a}{\tau_a} - G_a(n_a)N + P_a + P_{af} \qquad (1a)$$

$$\frac{dn_a}{dt} = -\frac{n_b}{\tau_b} - G_b(n_b)N + P_b + P_{bf} \qquad (1b)$$

$$\frac{dN}{dt} = [(1-h)G_a(n_a) + hG_b(n_b) - \Gamma]N \qquad (1c)$$

where

n_s $(s = a,b)$ are the uniform carrier densities in sections A or B,

N is photon density in the cavity

τ_s are carrier lifetimes,

P_s are injection rates,

Γ is the cavity loss,

h is the volume fraction of the absorbing section in the cavity,

$G_s(n_s)$ are the gain values related to corresponding carrier densities, where a linear approximation for the gain is used, that is

$G_s(n_s) = g_s(n_s - n_{s0})$, $g_s = \frac{\partial G}{\partial n}$ is the differential gain for section A or B.

$P_{af} = N \otimes h_a$ and $P_{bf} = N \otimes h_b$ are the carrier injection rates due to optoelectronic feedback, h_a, h_b are feedback impulse responses for sections A and B respectively and "$\otimes$" stands for convolution.

By use of the following substitution [1]:

$$x = g_a(1-h)(n_a - n_{a0})/\Gamma$$
$$y = g_b h(n_b - n_{b0})/\Gamma$$
$$z = g_a \tau_a N$$
$$\tau = t/\tau_a$$

these equations are reduced to the normalized equations:

$$\frac{dx}{d\tau} = -(x - x_0) - xz + \frac{1-h}{\Gamma}\tilde{h}_a(\tau) \otimes z(\tau), \qquad (2a)$$

$$\frac{dy}{d\tau} = -\frac{y - y_0}{\tilde{\tau}} - \gamma yz + \gamma \frac{h}{\Gamma}\tilde{h}_b(\tau) \otimes z(\tau), \qquad (2b)$$

$$\frac{dz}{d\tau} = \tilde{\Gamma}(x + y - 1)z \qquad (2c)$$

where $x_0 = g_a(1-h)(P_a\tau_a - n_{0a})/\Gamma$, $y_0 = g_b h(P_b\tau_b - n_{0b})/\Gamma$ are normalized injection rates to sections A and B respectively, $\tilde{\tau} = \tau_b/\tau_a$, $\gamma = g_b/g_a$ and $\tilde{\Gamma}$ is normalized cavity loss rate.

To find the equilibrium state (x_e, y_e, z_e) of the system described by the above equations, one should assume $\frac{dx}{d\tau} = \frac{dy}{d\tau} = \frac{dz}{d\tau} = 0$, and $z = z_e = const$. The feedback terms reduce to

$$\tilde{h}_a(\tau) \otimes z(\tau) = z_e \int_{-\infty}^{\infty} \tilde{h}_a(\tau)d\tau = z_e S_a,$$
$$\tilde{h}_a(\tau) \otimes z(\tau) = z_e \int_{-\infty}^{\infty} \tilde{h}_a(\tau)d\tau = z_e S_b$$

($\int_{-\infty}^{\infty} \tilde{h}_a(\tau)d\tau$ and $\int_{-\infty}^{\infty} \tilde{h}_b(\tau)d\tau$ are denoted as S_a and S_b respectively).

After introduction of $\hat{h}_a(\tau) = \frac{1-h}{\Gamma}\tilde{h}_a(\tau)$, $\hat{h}_a(\tau) = \gamma\frac{h}{\Gamma}\tilde{h}_b(\tau)$ equations for the equilibrium state of the system become

$$-(x_e - x_0) - x_e z_e + S_a z_e = 0,$$
$$-\frac{y_e - y_0}{\tilde{\tau}} - \gamma y_e z_e + S_b z_e = 0,$$
$$x_e + y_e - 1 = 0$$

which yields $x_e = \frac{x_0 + S_a z_e}{1 + z_e}$, $y_e = \frac{y_0/\tilde{\tau} + S_b z_e}{1/\tilde{\tau} + \gamma z_e}$ and a quadratic equation for z_e:

$$\tilde{\tau}(S_a\gamma + S_b - \gamma)z_e^2 + (S_a + \gamma\tilde{\tau}x_0 + \tilde{\tau}S_b + y_0 - \gamma\tilde{\tau} - 1)z_e + x_0 + y_0 - 1 = 0$$

In the problem under investigation $\hat{h}_a$ and $\hat{h}_b$ are the impulse responses of the band-pass filter used in the optical feedback. The corresponding transfer functions have zero DC

gain. The equilibrium state of the system with optoelectronic feedback is the same as that of the open-loop system without feedback, and is given by

$$z_e = \frac{1}{2\gamma\tilde{\tau}}\left[\gamma\tilde{\tau}(x_0-1)+y_0-1+\sqrt{(\gamma\tilde{\tau}(x_0-1)+y_0-1)^2+4\gamma(x_0+y_0-1)}\right], \quad (3a)$$

$$x_e = \frac{x_0}{1+z_e}, \quad (3b)$$

$$y_e = \frac{y_0}{1+\gamma\tilde{\tau}z_e} \quad (3c)$$

To investigate the system dynamics we will make use of linearization of the governing equations (2) in the vicinity of the equilibrium state (3), keeping feedback terms in (2 a,b) unchanged. The state equations for a system linearized in this way can be written in the form [7]:

$$\frac{d\varepsilon}{d\tau} = \mathbf{J}\varepsilon + \mathbf{f},$$

where $\mathbf{J} = \left[\frac{\partial F_i}{\partial \varepsilon_j}\right]_{\varepsilon=\mathbf{x}-\mathbf{x}_0=0}$ is the Jacobian of the system without feedback and $\mathbf{f} = \left[\hat{h}_a(\tau)\otimes z(\tau), \hat{h}_b(\tau)\otimes z(\tau), 0\right]^T$ is the feedback vector.

This gives the linearized governing equations:

$$\frac{dx}{d\tau} = (-1-z_e)x - x_e z + \hat{h}_a(\tau)\otimes z(\tau), \quad (4a)$$

$$\frac{dy}{d\tau} = (-\frac{1}{\tilde{\tau}} - \gamma z_e)y - \gamma y_e z + \hat{h}_b(\tau)\otimes z(\tau), \quad (4b)$$

$$\frac{dz}{d\tau} = \tilde{\Gamma}(x+y)z_e \quad (4c)$$

where the origin is moved to the equilibrium point (3) and the new state vector is denoted $(x, y, z)^T$ as before.

Taking the Laplace transform of both sides of each of the equations (4), one obtains:

$$(-\frac{x_0}{x_e} - s)X(s) - x_e Z(s) + \hat{H}_a(s)Z(s) = 0,$$

$$\left(-\frac{1}{\tilde{\tau}} - \gamma z_e - s\right)Y(s) - \gamma y_e Z(s) + \hat{H}_b(s)Z(s) = 0,$$

$$\tilde{\Gamma}\left[X(s) + Y(s)\right]Z_e - sZ(s) = 0$$

where *X(s), Y(s), Z(s)* are Laplace transforms of *x(t), y(t), z(t)* respectively and $\hat{H}_a(s)$ and $\hat{H}_b(s)$ are transfer functions of the feedback to sections 1 and 2 respectively.

The system above can be considered as a system of linear algebraic equations with respect to *X(s), Y(s), Z(s)* depending upon parameters *s*, $\hat{H}_a(s)$, $\hat{H}_b(s)$. It has a nontrivial solution if and only if the determinant of its matrix is zero, that is

$$det\begin{bmatrix} -\frac{x_0}{x_e} - s & 0 & -x_e + \hat{H}_a(s) \\ 0 & -\frac{1}{\tilde{\tau}} - \gamma z_e - s & -\gamma y_e + \hat{H}_b(s) \\ \tilde{\Gamma} z_e & \tilde{\Gamma} z_e & -s \end{bmatrix} = 0$$

which gives the following equation:

$$s^3 + \left(\frac{1}{\tilde{\tau}} + \gamma z_e + \frac{x_0}{x_e}\right)s^2 + \left[\tilde{\Gamma} z_e \gamma y_e + \frac{x_0}{x_e}\left(\frac{1}{\tilde{\tau}} + \gamma z_e\right) + \tilde{\Gamma} z_e x_e\right]s + \tilde{\Gamma} z_e\left[\gamma y_e \frac{x_0}{x_e} + x_e\left(\frac{1}{\tilde{\tau}} + \gamma z_e\right)\right] -$$
$$- \tilde{\Gamma} z_e\left(\frac{x_0}{x_e} + s\right)\hat{H}_b(s) - \tilde{\Gamma} z_e\left[\left(\frac{1}{\tilde{\tau}} + \gamma z_e\right) + s\right]\hat{H}_a(s) = 0 \qquad (5)$$

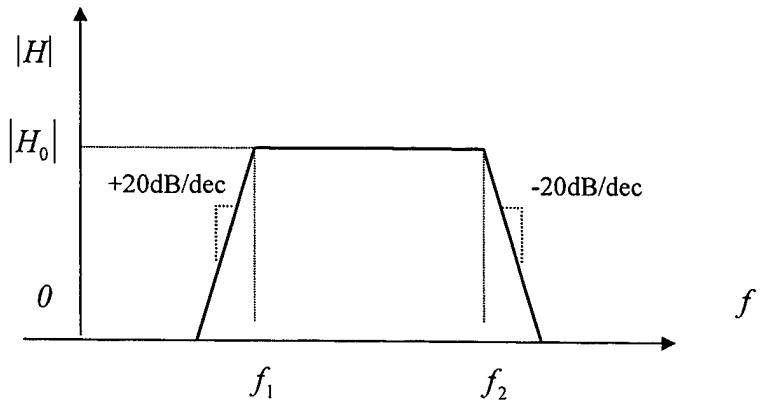

Fig. 2 Bode Plot for wide-band bandpass filter transfer function.

We assume that the transfer functions of the amplifiers $\hat{H}_a(s)$ and $\hat{H}_b(s)$ are chosen to be wide-band band-pass transfer functions with corner frequencies f_1 and f_2, that is [9]

$$\hat{H}_i(s) = H_{0i} \frac{j\dfrac{s}{s_{1i}}}{\left(1+j\dfrac{s}{s_{1i}}\right)\left(1+j\dfrac{s}{s_{2i}}\right)} = \hat{H}_{0i} \frac{s}{1+\beta_i s-\alpha_i s^2}, \qquad (6)$$

where $s_1 = 2\pi f_1$, $s_2 = 2\pi f_2$, $\alpha = \dfrac{1}{s_{1i}s_{2i}}$, $\beta = \left(\dfrac{1}{s_{1i}}+\dfrac{1}{s_{2i}}\right)j$, and

$$\hat{H}_{0i} = j\tau_a^{-1} H_{0i} f_{1i}^{-1} e^{sT} \qquad (7)$$

The factor e^{sT} accounts for delay time T across the feedback loop. With the transfer function given in Eq. (7), Eq. (5) yields a nonlinear algebraic equation with respect to s. If we introduce

$$A=1,$$

$$B=\frac{1}{\widetilde{\tau}}+\gamma z_e+\frac{x_0}{x_e},$$

$$C=\widetilde{\Gamma} z_e \gamma y_e+\frac{x_0}{x_e}\left(\frac{1}{\widetilde{\tau}}+\gamma z_e\right)+\widetilde{\Gamma} z_e x_e,$$

$$D=\tilde{\Gamma} z_e\left[\gamma y_e \frac{x_0}{x_e}+x_e\left(\frac{1}{\tilde{\tau}}+\gamma z_e\right)\right]$$

(5) can be rewritten in the form

$$\left(As^3+Bs^2+Cs+D\right)\left(1+\beta s-\alpha s^2\right)-\tilde{\Gamma} z_e\left(\frac{x_0}{x_e}s+s^2\right)\hat{H}_{0b}-\tilde{\Gamma} z_e\left[\left(\frac{1}{\tilde{\tau}}+\gamma z_e\right)s+s^2\right]\hat{H}_{0a}=0$$

and after reduction

$$\sum_{i=0}^{5} C_i s^i = 0 \qquad (8)$$

where

$$\begin{aligned}
C_0 &= D,\\
C_1 &= C+\beta D-\tilde{\Gamma} z_e\left(\frac{1}{\tilde{\tau}}+\gamma z_e\right)\hat{H}_{0a}-\tilde{\Gamma} z_e \frac{x_0}{x_e}\hat{H}_{0b},\\
C_2 &= B+\beta C-\alpha D-\tilde{\Gamma} z_e \hat{H}_{0a}-\tilde{\Gamma} z_e H_{0b},\\
C_3 &= A+\beta B-\alpha C\\
C_4 &= \beta A-\alpha B,\\
C_5 &= -\alpha A
\end{aligned} \qquad (9)$$

Roots of equation (8)-(9) can be found numerically for different combinations of system parameters ($x_0, y_0, \gamma, \tilde{\Gamma}, \tilde{\tau}$) and different feedback parameters (the gain, corner frequencies). A MatLab script (LAN.M) has been written for this purpose. Its listing is given in the appendix B.

Depending upon complex values of s the phase trajectories of the linearized system (4) can be one of several known types: cycle, saddle node, center etc. ([7] chapter I). As certain parameters of the nonlinear system (2) are being changed (e.g. x_0), it appears to be structurally unstable [8], that is, the shape of the phase trajectories changes qualitatively and the system described by (2) may go through one or more bifurcation points, giving rise to periodic orbits on the phase diagram of the system. The left-hand side of the characteristic equation for the system without feedback is a polynomial with real coefficients and, as it is stated in [1], the system undergoes *Hopf* bifurcation [8], that is, exactly two of three eigenvalues of the system change the signs of their real parts from

minus to plus. In the case of the transfer function given by (6) with a nonzero delay time, the left-hand side of (5) is a transcendent complex function of complex argument s, and the behavior of the roots and nature of the bifurcation is not so clear as in the case presented in [1].

It is clear however, that the system can have a periodic solution only if the corresponding linearized system has an infinitely growing solution. Indeed, the nonlinear terms in (2a,b) are infinitely small of the second order in the vicinity of the equilibrium point and have an effect on the system behavior only comparatively far (in the state space) from the equilibrium point. A solution of (2) starting from inside a small vicinity of the equilibrium point is very close to the solution of system (4) and, if the latter is tending to zero, Eq. (2) will also converge to the equilibrium point. That is why one can expect the system described by (2) to undergo SSP only if one or more of the eigenvalues of (4) have positive real part.

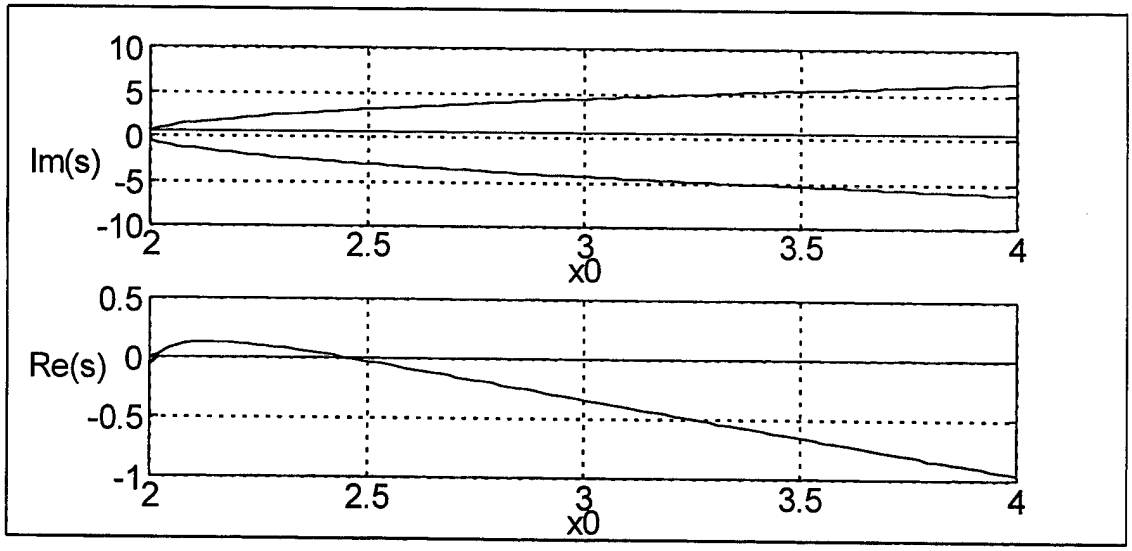

Fig. 3a Real and imaginary parts of roots of eq. (8)-(9) for the system without feedback.

Fig.3 represents the plot of real and imaginary parts of roots of equation (8)-(9) versus x_0 generated by program LAN.M for the case of the system without feedback (Fig. 3a) and with feedback (Fig. 3b). The fourth and fifth roots have large negative real

parts and not shown on Fig.3. As it can be seen from Fig.3, at $H_0 \neq 0$ there are regions on x_0-axis where one or two roots have positive real parts. In the case of the system without feedback (8) has two complex-conjugate roots and one negative real root. To find out more exactly what is the condition for SSP to exist the numerical simulation has been used.

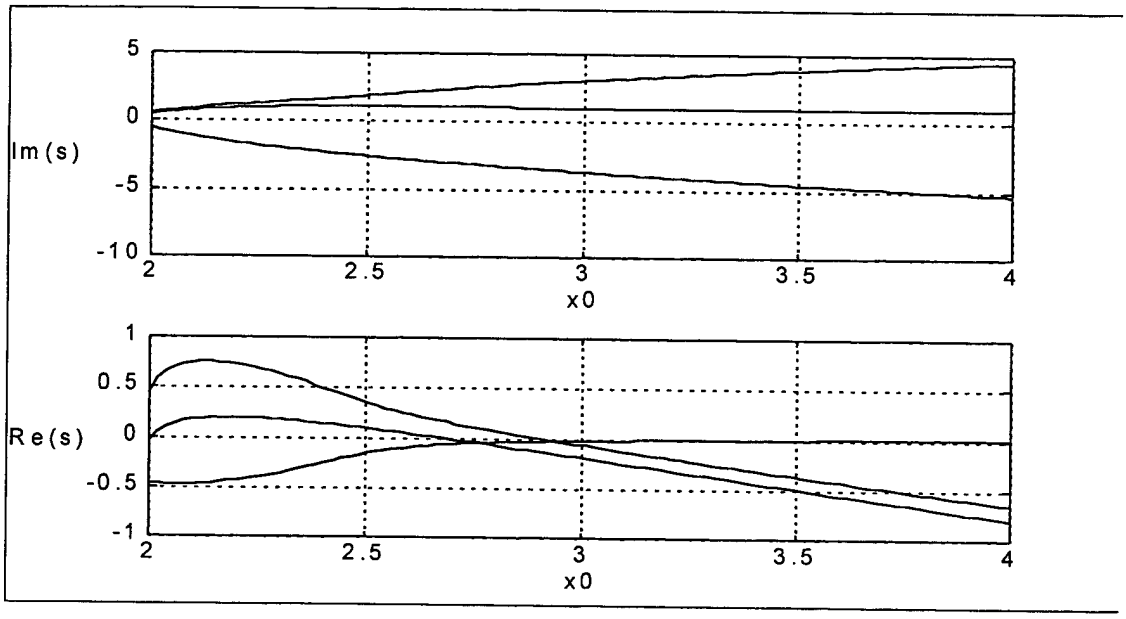

Fig. 3b Example of real and imaginary parts of roots of eq. (8) for the system with feedback.

Fig.3 also shows that in the case of nonzero feedback gain, the domain of pulsation extends longer along x_0 axis than in the case of the system without feedback.

2.2 Effect of the feedback on SSP frequency.

In certain situations the imaginary parts of roots of equation (6) can be used as rough estimates for the SSP frequency in the vicinity of the bifurcation point. This is because (2) can be expected to have solutions close to solution of linearized equation (4), and near the bifurcation point the form of the phase trajectories for (4) are cycles [8].

In the case of no feedback the system undergoes Hopf bifurcation, and Fig.3 shows that imaginary parts of the pair of complex conjugate roots increase as x_0 increases [1]. As indicated in [2], it has been found empirically that the frequency of oscillations in semiconductor LD is proportional to square root of injection rate. This increase in SSP frequency can also be observed qualitatively both on Fig.3 ($\mathrm{Im}(s) \approx \Omega = 2\pi f$) and in the numerical simulation, though quantitative agreement between frequencies predicted by Fig.3 and the results of the simulation is only in the order of magnitude.

In the case of the system with feedback behavior of the roots of (6) is rather complex and their imaginary parts can hardly be used as more or less accurate estimates for the SSP frequency.

General considerations make it possible, however, to predict certain characteristic features of the behavior of the SSP frequency for the system with feedback of nonzero delay time.

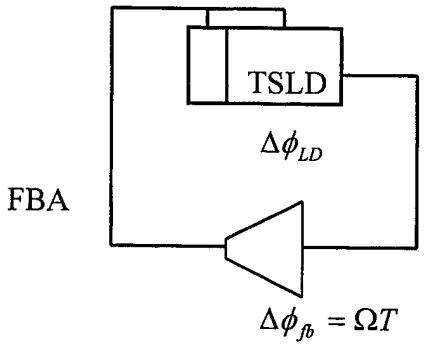

Fig. 4 Phase change for the signal in the system with feedback.

The closed-loop system is schematically shown on Fig.4. If the feedback gain is chosen so that the feedback signal is large enough, the oscillation in the TSLD cavity can become amplified, attenuated, or completely extinct depending upon the phase shift between the pulsation in the cavity and the feedback signal. The condition under which the feedback signal supports the oscillations is, as it can be seen from Fig. 4,

$$\Delta\phi_{LD} + \Omega T = 2\pi N \qquad (10)$$

where N is an integer.

SSP is expected to have maximum amplitude at frequencies

$$F_N = \frac{N}{T} - \frac{\Delta\phi_{LD}}{2\pi T} \qquad (11)$$

If $\Delta\phi_{LD}$ is small enough, SSP will occur only within frequency bands centered at F_N with gaps between them. The width of these bands will depend upon the rate of change of $\Delta\phi_{LD}$ with respect to frequency. This may cause the frequency versus x_0 plot to have the appearance of frequency "steps" spaced in frequency by $\frac{1}{T}$, as it follows from (11).

These simple considerations make possible to predict only qualitatively the discreet, step-like appearance of SSP frequency versus injection rate dependence but do not provide any reliable information about the allowed and forbidden band's width, the amplitude of SSP etc.

To obtain this information, either experiment or numerical simulation should be used.

3. Numerical simulation and results

To prove the existence of SSP and verify certain results predicted by the theory presented in the previous section we make use of direct simulation of SSP in the two-sectional laser diode with optoelectronic feedback. Program FSP has been written for this purpose in Fortran. It integrates a system of nonlinear normalized state equations of the TSLD (2) using Runge-Kutta method (routine ODEINT is supplied in the Numerical Recipes for MS-FORTRAN, [12]) and outputs the solutions $[x(t), y(t), z(t)]^T$ into a file.

To introduce the feedback terms, the impulse response of the feedback has been calculated by use of a standard Fast Inverse Fourier Transform routine (FOUR1) supplied in the Numerical Recipes for MS-FORTRAN and described in [12]. Numerical integration is used to calculate the convolution. Impulse response corresponding to the transfer function described by (6) is shown on Fig. 5d and the typical appearance of the solution generated by FSP is shown on Fig. 5 a,b,c. Listing of FSP is given in the appendix A.

As a practical example we have chosen the TSLD consisting of an amplifying section and an absorbing section. The difference in amplifying properties of the sections was achieved by applying injection currents of differing signs: x_0 for the amplifying section and y_0 for the absorbing section. The device parameters have been chosen to be consistent with the experimental device used previously [1]: cavity volume $V = 250 \times 4 \times 0.2\ \mu m$, h=0.10, $\tau_a = 2$ ns, $\tilde{\tau} = 0.606$, $n_{0a} = 1.2 \times 10^{18}$ cm^{-3}, $n_{0b} = 2.4 \times 10^{18}$ cm^{-3}, $\Gamma = 6.25 \times 10^{11}$ s^{-1}, $g_{0a} = 4.5 \times 10^{-7}$ cm^3 / s, $g_{a0} / g_{b0} = 0.325$, wavelength of the laser radiation $\lambda = 1300$ nm.

The feedback loop parameters have been chosen so that (6) represents a wide-band band-pass transfer function with a supposed SSP frequency estimated from Fig. 3 well inside the pass band of the amplifier at all allowable values of x_0. We have chosen $f_1 = 0.1$ $f_2 = 5.0$ units of normalized frequency which corresponds to corner frequencies of the feedback amplifier of 50 MHz and 2.5 GHz respectively. This makes the

feedback transfer function flat enough in the frequency range in which SSP is anticipated to occur.

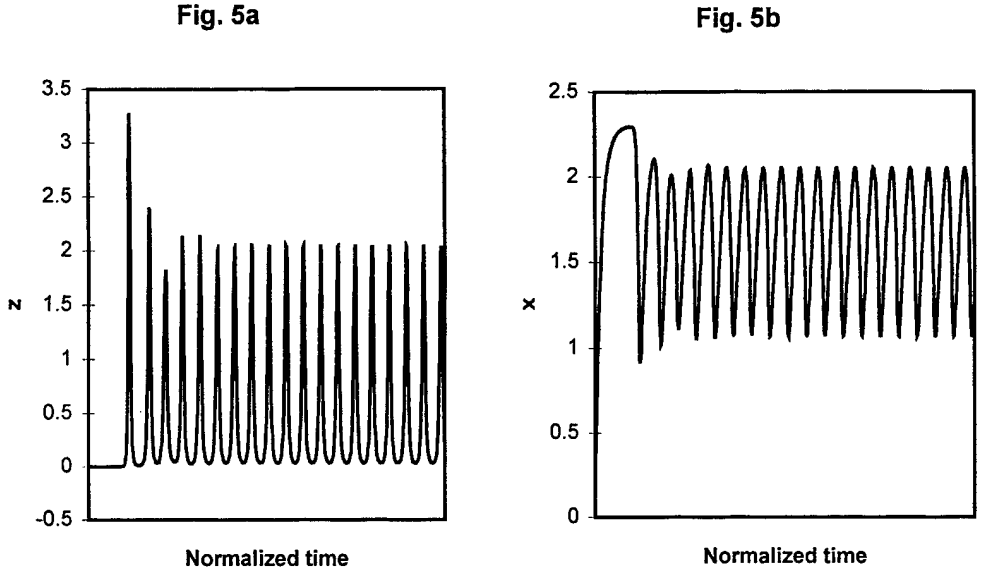

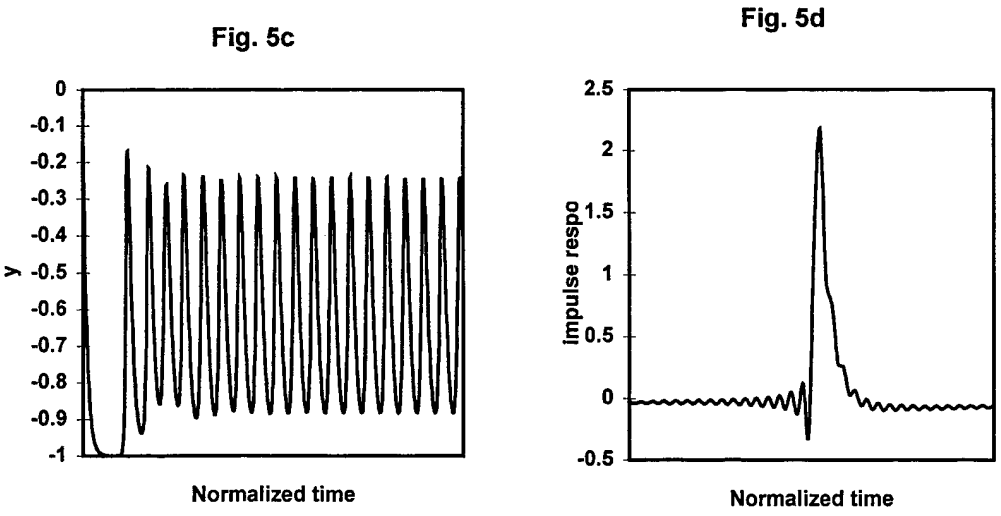

Fig. 5 Typical dynamics of FSP (5a-c) with impulse response given as in 5d.

The net feedback Gain $\hat{H}_0$ (i.e. the ratio between the average photon density N in the cavity and injection rate density due to the feedback) can be varied by choice of proper amplifier gain G. In the present case, it has been chosen so that peak values of

feedback output current are less than or equal to the DC injection current. The photodetector sensitivity was assumed R = 0.1 mA/mW, and the group refraction index inside the cavity is assumed to be $n_g = 3.4$. Then the normalized net gain is given by

$$\hat{H}_{0a} = H_{0a}\frac{1-h}{(\Gamma/V)\tau_a} = \frac{1}{4}\frac{1}{f_1}v_g\alpha_{mir}h\nu RG\frac{1-h}{(\Gamma/V)\tau_a}.$$

In the case of Fabry-Perot LD $\alpha_{mir} = \frac{1}{2L}\ln\frac{1}{R_1R_2}$-cavity loss rate, $R_1 = 1$, $R_2 = \left(\frac{n-1}{n+1}\right)^2$ are the mirror reflectivities [10], and $\hat{H}_{a0}$ must satisfy the condition

$$\hat{H}_0 N_{peak} \cong P_a. \qquad (12)$$

At $x_0 = 2.1$ the DC injection rate density $P_a \approx 2\times10^{27}$ $s^{-1}cm^{-3}$ and (12) yields $H_{0a} \cong 0.1....0.5$ which corresponds to the feedback current amplifier gain $G \cong (1...5)\times10^3$.

The first issue subjected to verification was the region of existence of SSP. As it was anticipated, several (at least one) root of equation (8)-(9) must have a positive real part for SSP to exist. To find out more exactly the number of such roots, the numerical simulation has been used. Fig.6 presents the simulated value of the boundary point at which SSP ceases to exist (i.e. $z(t)$ becomes decaying with time), plotted with respect to net feedback gain (curve 1). In this figure the area between the curves 2 and 3 represents the region where the linearized system has exactly one eigenvalue with positive real part. The area below the curve 3 corresponds to a linearized system with more than one "unstable" eigenvalue and the area above the curve 2 corresponds to a stable linear system.

Curves 2 and 3 have been generated with aid of the program LAN.

Fig. 6

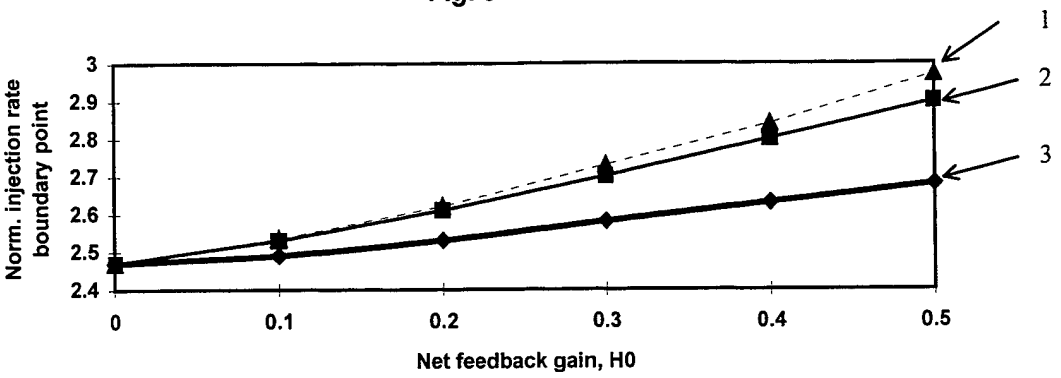

Fig. 6 Boundary points at which SSP cease to exist.

As one can observe from Fig.6, the original nonlinear system (2) grows unstable and undergoes SSP at values of x_0 very close to those at which the linearized system described by (4) becomes unstable. The difference between curves 1 and 2 is attributed to the finite width of the frequency "window" used for numerical calculation of the impulse response of the feedback loop, which causes curve 1 to shift up with respect to what it would be if a nonzero value of the feedback transfer function at large values of frequency is taken into account.

Fig.7

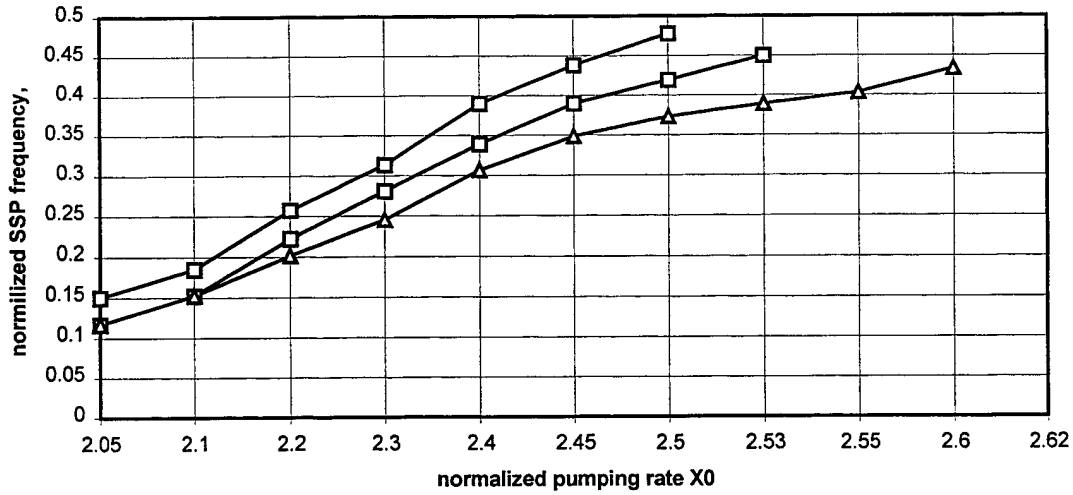

Fig. 7 SSP frequency as a function of the normalized pumping rate.

The effect of the optoelectronic feedback on the SSP frequency has also been investigated for the feedback loop with different net gain and delay time. In case of zero delay time T in (7) the simulation shows monotonic growth for SSP frequency as x_0 increases (Fig.7), which is in qualitative agreement with the results presented in [2] and mentioned above.

If the delay time across the feedback loop is taken into account, then according to (10) SSP must exist within bands centered at the frequencies f_N given by (10). Simulated SSP frequency and amplitude for the net feedback gain $\hat{H}_0 = 0.3$ and normalized feedback delay time $T = 5$ are plotted on Fig.8 and Fig.9 respectively.

Fig. 8

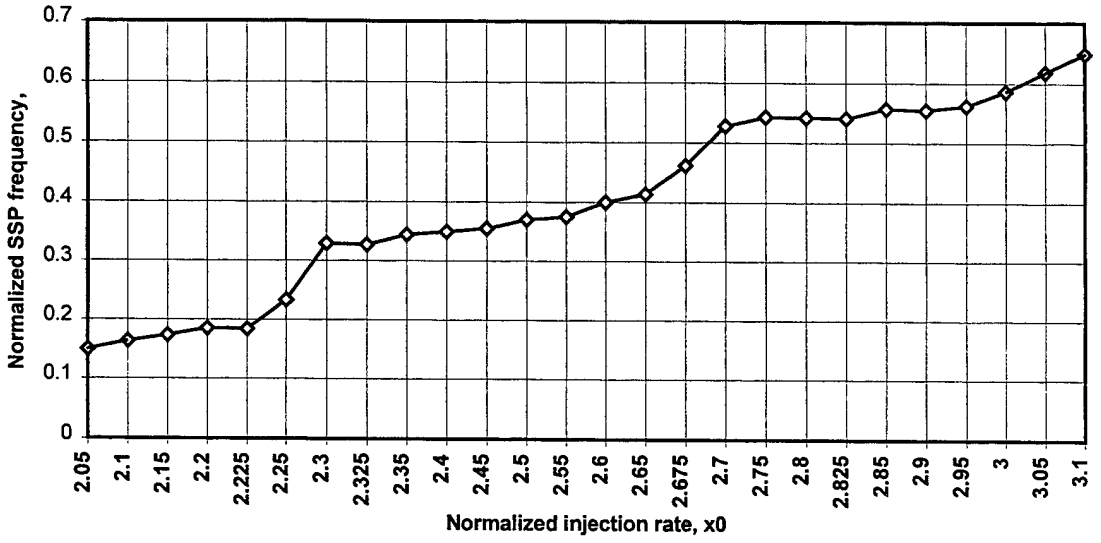

Fig. 8 SSP frequency as a function of the normalized pumping rate with delayed feedback.

As it was expected, the frequency dependence on the normalized injection rate x_0 has characteristic appearance of frequency "steps" whereas the pulsation amplitude versus x_0 plot consists of several bands where SSP exists and its amplitude grows monotonically as x_0 increases and the character of this growth is close to linear. These bands are separated by regions where SSP is suppressed by the effect of feedback as described above.

Fig.9

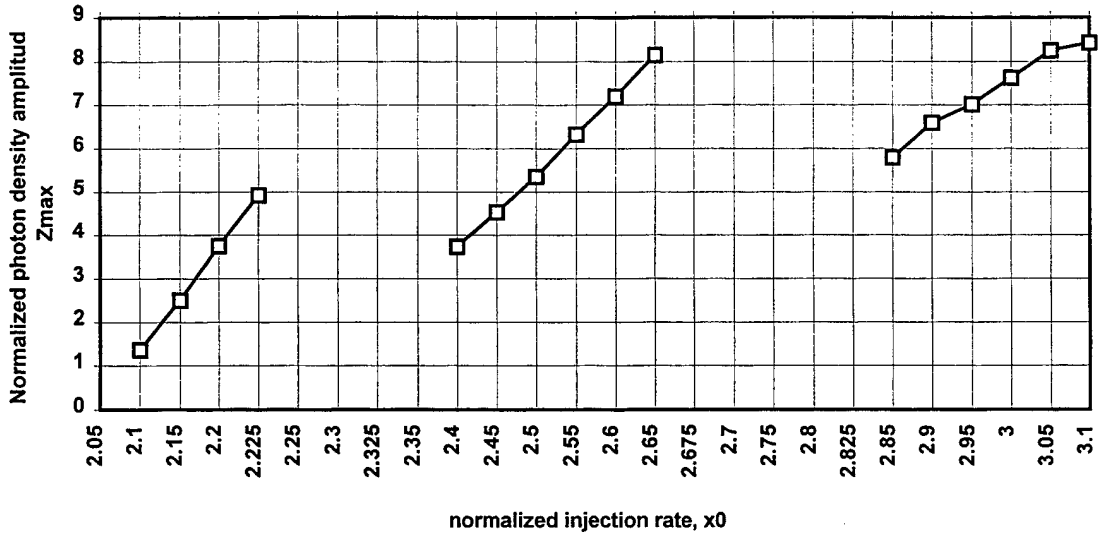

Fig. 9 Amplitude of the normalized photon density as a function of the normalized injection rate.

Such a frequency versus injection rate relationship may be used in lightwave communication networks with subcarrier multiplexing (SCM). In systems of this kind users are assigned certain subcarrier frequencies [1],[6]. In our case each user can use a frequency band coincident with one of the frequency "steps" where the frequency versus injection current curve is more or less flat (Fig.8) and the amplitude modulation of the subcarrier will cause relatively small frequency chirp of the modulated signal.

Fig.10

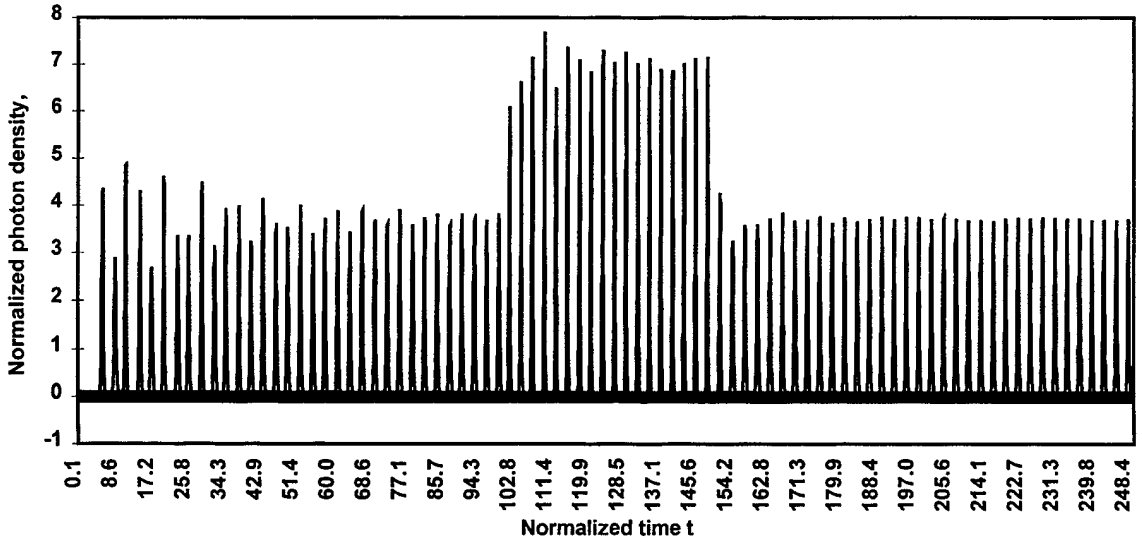

Fig. 10 Amplitude modulation of the FSP subcarrier.

Fig. 10 presents a simulated example of amplitude modulation of the subcarrier by a rectangular pulse generated by a slightly modified version of the program FSP. This pulse may represent, for example, a bit transmitted through a digital communication network. In this example the LD is biased close to the middle of central "step" of Fig. 8-9. The normalized injection rate x_0 is switched during the modulation from 2.40 to 2.60 and then back to 2.40, giving rise to a pulse in the light output of the laser (Fig. 10). The front and rear edges of the pulse are shown on Fig.11 a, b to determine the rise and fall times of the pulse.

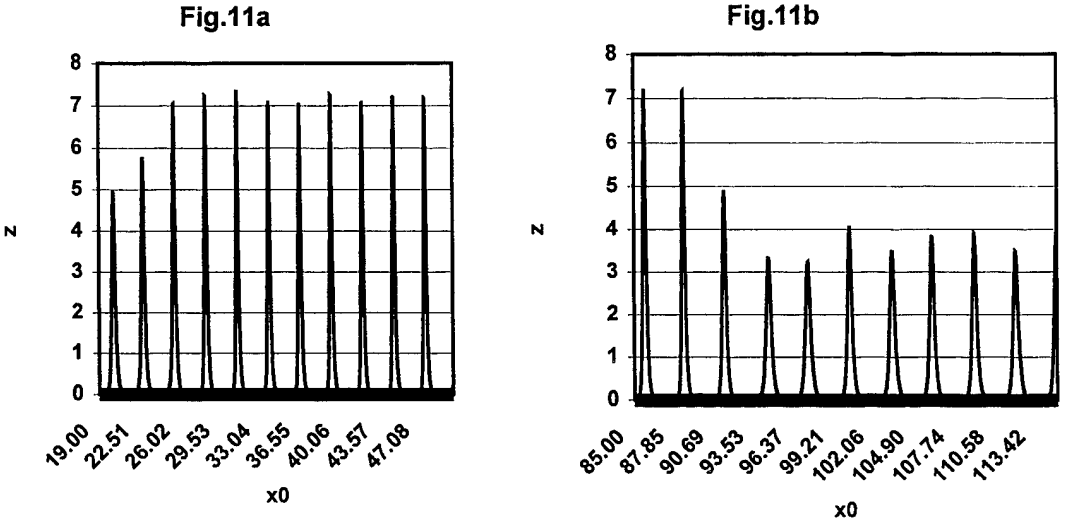

Fig. 11 Rise and fall transients of FSP amplitude modulation.

As can be concluded from Fig.11 a, b, characteristic switching times for the laser light output are of the order of 5-10 nanoseconds. This corresponds to possible transmission bit rate of the order of hundreds Mb/s.

4. Conclusion

Investigation of Self-Sustained Pulsation in the semiconductor laser diode with optoelectronic feedback has been presented. Numerical and analytical techniques have been used to investigate stability of the semiconductor LD consisting of amplifying and absorbing sections with wide-band band-pass feedback, and to investigate the conditions of existence for SSP and study its characteristics.

The main results can be formulated as follows. First, it has been shown by analytical stability analysis that within a certain range of LD and feedback parameters the linearized system corresponding to the system of rate equations (2) exhibits structural instability. This phenomenon is the origin for the Self-Sustained Pulsation of the LD described by (2). The boundary points of the SSP region in the space of the system parameters have been found by the stability analysis. Second, the step-like behavior of SSP frequency with respect to LD injection rate for the system with nonzero feedback delay time has been predicted on the basis of the closed-loop amplifier model and its major characteristics have been found.

In numerical simulation, the system of normalized rate equations (2) has been solved numerically and the solution has been investigated at a variety of LD and feedback parameters. The boundary values for the instability regime have been found to be in good agreement with those predicted by the stability analysis. Second, SSP frequency and amplitude dependence upon injection rate have been studied. It has been found for the system with nonzero feedback delay time that the instability region consists of several allowed frequency bands where the SSP amplitude varies at an almost constant rate separated by bands of decaying oscillations, which causes the frequency versus injection rate curve to have a characteristic step-like appearance. This makes it possible to modulate the SSP amplitude introducing relatively low change into its frequency if the LD bias point is chosen within one of such "steps". This performance probably can make the two-sectional laser diodes with optoelectronic feedback useful as tunable subcarrier sources for high-speed lightwave communication networks with subcarrier multiplexing.

Appendix A

```
C*********************************************************
C*                                                       *
C*                      PROGRAM FSP                      *
C*                                                       *
C*  Dynamics of SSP laser diode With Optoelectronic feedback *
C*                        RIT,1996                       *
C*********************************************************
C
C
C
C
      PARAMETER (NVAR=3,NMAX=50,KMAXX=1000,MSTEP=200000,BRK=4)
      IMPLICIT REAL (A-H,O-Z)
      DIMENSION YSTART(NVAR),xp(KMAXX),yp(NMAX,KMAXX),yt(NVAR,MSTEP),
     *                        H(MSTEP),TF(MSTEP)
      COMMON /SSPLD/ TAU_B1,GAMMA1,TAMMA1,X10,Y10,FB1,EICH
      COMMON /ODE/ t1,t2,eps,h1,HMIN,nok,nbad,N
      COMMON /path/ kmax,kount,dxsav,xp,yp
      COMMON /FILDATA/DELTA_F,S1,S2,H0,F1,F2,TETA
      COMPLEX FUNC,Ji
      COMPLEX TRAN_F,SINC
      EXTERNAL derivs,bsstep,FILTERH
      EXTERNAL TF_RE,TF_IM,TRAN_F,SINC
C     Get parameters (SSP LD and computational)
C
        EICH=0.1
        Ji=CMPLX(0.0,1.0)
C
        CALL GETPAR          !   Initialize the SSP Laser Diodes and Feedback.
C
        kmax=100
        DO 10 I = 1,NVAR
        YSTART(I)  = 0.0001
  10    CONTINUE
C
C     Integration over the interval (t1,t2)
C
        NN=(t2-t1)*(F2-F1)              !Time-domain mesh
        NF=NN*2
        DELTA_t=(t2-t1)/NN
        DELTA_F=1/(2*(t2-t1))           !Frequency-domain mesh
C
        x1=0
        x2=0
        dxsav=DELTA_t/50
C
C
C       Calculating the impulse response
C
```

```
      DO 14 J=1,NN
            H(J)=0.0
            TF(2*J-1)=0.0
            TF(2*J)=0.0
 14   CONTINUE

      DO 11 J=0,NF-1                !Setting up the transfer function array

            FUNC=TRAN_F(J)
            TMP=REAL(FUNC)
            TF(2*J+1)=TMP
            TF(2*J+2)=IMAG (FUNC)
 11   CONTINUE
C
C
C
      CALL FOUR1(TF,NF,1)           !Calculating Inverse Fourier Transform, subroutine FOUR1
                                    ! from   Numerical Recipes
C
      DO 13 J=1,NN                                  !Picking up values of  impulse response
            FI=-3.14159*(F2-F1)*DELTA_T*(J-1)       !Canceling quickly oscillating factor
            H(J)=TF(2*J-1)*COS(FI)-TF(2*J)*SIN(FI)
 13    CONTINUE
C
      DO 17 J=1,NN                  !Inverse Fourier Transform finally
            H(J)=H(J)*DELTA_F
 17   CONTINUE
C
C
       DO 20 JJ=1,NN
            x1=x2
            x2=x1+DELTA_t
C
      FB1=0.0
      DO 12 N=1,JJ
      FB1=FB1+yt(3,N)*H(JJ-N)       !Value of convolution for the moment JJ
 12   CONTINUE
      FB1=FB1*DELTA_t

      CALL odeint(YSTART,NVAR,x1,x2,eps,h1,hmin,nok,nbad,
     *      derivs,bsstep)          !Produce the solution of LD equations for JJth step
C                                   !Subroutine ODEINT from Numerical recipes
      DO 15 I = 1,NVAR
            yt(I,JJ) = YSTART(I)
 15   CONTINUE
C
 20   CONTINUE
C
C
      OPEN (1,FILE='ssp.out',STATUS='UNKNOWN')    !Output the result to a file
      DO 99 I=1,(NN/BRK)
            J=I*BRK
            WRITE (1,100) REAL(J)*DELTA_t, yt(1,J), yt(2,J), yt(3,J),H(J)
 99   CONTINUE
```

```
C
      CLOSE (1)
C
 100  FORMAT (1X,F8.4,2X,3F14.6,2X,F16.8)
C
   STOP
   END
C
   SUBROUTINE GETPAR
C  ---------- ------
C
C  Get laser diode, feedback and odeint parameters and store them in common blocks SSPLD, FILDATA
C  and ODE respectively.
C
C
   IMPLICIT REAL (A-H,O-Z)
   COMMON /SSPLD/ TAU_B1,GAMMA1,TAMMA1,X10,Y10,FB1,EICH
   COMMON /ODE/ t1,t2,eps,h1,HMIN,nok,nbad,N
   COMMON /FILDATA/DELTA_F,H0,S1,S2,F1,F2,TETA
   OPEN (1,FILE='ssp.in',STATUS='OLD')
C
C  TSLD  parameters.
C
   READ (1,*) TAU_B1          !Carrier lifetime ratio
      READ (1,*) GAMMA1       !gain ratio
      READ (1,*) TAMMA1       !Normalized photon lifetime
      READ (1,*) X10          !Normalized pumping rate in section A
      READ (1,*) Y10          !Normalized pumping rate in section B
C
C  ODEINT parameters
C
      READ (1,*) t1           !starting point of integration
      READ (1,*) t2           !end point of integration
      READ (1,*) eps          !starting point of integration
      READ (1,*) h1           !initial step size
      READ (1,*) HMIN                 !minimum allowable step size (0.1 ps)
C
C      FEEDBACK Parameters
C
      READ (1,*) H0           !Feedback gain
      READ (1,*) S1           !Feedback lower frequency
      READ (1,*) S2           !Feedback upper frequency
C
C
      READ (1,*) N            !Total integration steps=2**N
      READ (1,*) F1           !Frequency region lower frequency
      READ (1,*) F2           !Frequency region upper frequency
      READ (1,*) TETA         !Feedback delay time
C
   CLOSE (1)
C
   RETURN
   END
C
```

```
      SUBROUTINE derivs(T,Y,DYDT)
C     ------ -------- -
C
C     Rate equations for two coupled SSP laser diode with optoelectronic feedback.
C     For a description of parameters, see subroutine GETPAR.
C
C
      IMPLICIT REAL (A-H,O-Z)
      DIMENSION Y(3),DYDT(3)
      COMMON /SSPLD/ TAU_B1,GAMMA1,TAMMA1,X10,Y10,FB1,EICH
      COMMON /FILTDATA/DELTA_T,A,W0,IORDER
C
C     Rate equations for the TSLD .
C

          DYDT(1) = -(Y(1)-X10)-Y(1)*Y(3)+(1-EICH)*FB1
          DYDT(2) = -(Y(2)-Y10)/TAU_B1-GAMMA1*Y(2)*Y(3)+EICH*FB1
          DYDT(3) = TAMMA1*(Y(1)+Y(2)-1.0)*Y(3)
          RETURN
      END
C
C
```

Appendix B

```
%*****************************************
%*                                       *
%*                LAN.M                  *
%*    Stability analysis for SSP laser diodes *
%*                RIT, 1996              *
%*****************************************

x01 = 2.0                       %
x02 = 4.0                       %       Starting and ending values for x0

Gain_a = 0.3                    %       Net gain to sections A
Gain_b = Gain_a                 %       and B

f1 = 0.1                        %       Filter corner  frequencies
f2 = 5.0
gamma = 1/0.325         %       TSLD parameters
taub1 = 1.65
tau_ph = 1E-12
tau_e = 1E-09
Gtilda = 20.0
h = 0.1
y0 = -1

s1 = f1*2*pi
s2 = f2*2*pi

alfa = 1/(s1*s2)                %       Calculation of feedback parameters
beta = (1/s1+1/s2)*j
tau_r = tau_ph/tau_e
taub = 1/taub1
Ha0 = j*(1-h)*Gain_a
Hb0 = j*h*Gain_b*gamma

for i=1:100,                                            %       Loop for eigenvalues of (8)-(9)
        x0=x01+((x02-x01)/100)*i;

Di = sqrt((gamma*taub*(x0-1)+y0-1)^2+4*gamma*taub*(x0+y0-1))
ze = (1/(2*gamma*taub))*(gamma*taub*(x0-1)+y0-1+Di);
xe = x0/(1+ze);                                         %       Equilibrium points
ye = y0/(1+gamma*ze*taub);

A = +1;
B = x0/xe+taub1+gamma*ze;
C = (x0/xe)*(taub1+gamma*ze)+Gtilda*ze*ye*gamma+Gtilda*ze*xe;
D = Gtilda*ze*(ye*gamma*x0/xe+xe*(taub1+gamma*ze));


c5 = -alfa*A;
c4 = beta*A-alfa*B;
```

```
c3 = A+beta*B-alfa*C;
c2 = B+beta*C-alfa*D-Gtilda*ze*Ha0-Gtilda*ze*Hb0;
c1 = C+beta*D-Gtilda*ze*(taub1+gamma*ze)*Ha0-Gtilda*ze*(x0/xe)*Hb0;
c0 = D;
        c=[c5,c4,c3,c2,c1,c0];
        r=roots(c);
        im_koren1(i)=imag(r(1));                    %       Roots of the characteristic equation
        im_koren2(i)=imag(r(2));
        im_koren3(i)=imag(r(3));
        im_koren4(i)=imag(r(4));
        im_koren5(i)=imag(r(5));

        re_koren1(i)=real(r(1));
        re_koren2(i)=real(r(2));
        re_koren3(i)=real(r(3));
        re_koren4(i)=real(r(4));
        re_koren5(i)=real(r(5));

end


y=linspace(x01,x02,100)

 subplot(2,1,1)                                     %       Plotting
 plot(y,im_koren3,y,im_koren4,y,im_koren5)
 ylabel('Im(s)')
 xlabel('x0')
 grid
 subplot(2,1,2)
 plot(y,re_koren3,y,re_koren4,y,re_koren5)
 ylabel('Re(s)')
 xlabel('x0')
 grid
```

References

1. X. Wang, G. Li, C. Ih. "Microwave/millimeter-wave frequency subcarrier lightwave modulations based on self-sustained pulsation of laser diode", *IEEE J. Of Lightwave Technology*, vol 11, No. 2, pp. 309-314, February 1993.
2. K. Y. Lau, A. Yariv "Self-sustained picosecond pulse generation in a GaAlAs laser at an electrically tunable repetition rate optoelectronic feedback", *Appl. Phys. Lett.*, 45(2), pp 124-126, July 1984.
3. G. Li, R. Boncek, X. Wang and D. Sackett " Transient and optoelectronic feedback-sustained pulsation of laser diodes at 1300 nm", *IEEE Photonics Technology Letters*, Vol. 7, No. 8, pp. 854-856, August 1995.
4. Y. Simler, J. Gamelin and Sh. Wang "Pulsation stabilization and enhancement in self-pulsating laser diodes", *IEEE Photonics Technology Letters*, Vol. 4, No. 4, pp. 329-332, April 1992.
5. J.B. Georges and K. Y. Lau, "800 Mb/s Microwave FSK using a self pulsating compact disk laser diode," *IEEE Photonics Technology Letters*, vol. 4, no. 6, pp. 662-665, 1992.
6. J.B. Georges and K. Y. Lau, " Self-pulsating laser diodes as fast-tunable (<1 ns) FSK transmitters in subcarrier multiple-access networks," *IEEE Photonics Technology Letters*, vol. 5, no. 2, pp. 242-245, 1993.
7. Hassan Khalil, Nonlinear systems, Prentice Hall, Upper Saddle River, NJ, 1996
8. J. M. T. Thompson Nonlinear dynamics and chaos: geometrical methods for engineers and scientists, Wiley, New-York, 1987
9. Sergio Franco, Design with operational amplifiers and analog integrated circuits, McGraw-Hill, New-York, 1988
10. Gowind Agrawal Fiber-optics communication ststems, John Wiley & Sons, New-York, 1992.
11. H. Joseph Weaver, Applications of discrete and continuous Fourier-analysis, Krieger Publishing Company, Malabar, Florida, 1992

12. William H. Press, Brian P. Flannery, Saul A. Teukolsky and William T. Vetterling, Numerical Recipes: The art of scientific computing. Cambrige University Press, 1986
13. IMSL math/library: FORTRAN subroutines for mathematical applications. User's manual. Visual Numerics, 1994.